LA-UR- 97-1126

CONF-970670--4

Title:

CFD Analysis and Experimental Investigation Associated with the Los Alamos Nuclear Materials Storage Facility

Author(s):

J. D. Bernardin
S. M. Hopkins
W. S. Gregory
L. Parietti
D. H. Bultman
R. A. Martin

Submitted to:

1997 American Society of Mechanical Engineers Fluids Engineering Division Summer Meeting
Vancouver, British Columbia, Canada
June 22 - 26, 1997

HH

DISCLAIMER

CFD Analysis and Experimental Investigation associated with the Design of the Los Alamos Nuclear Materials Storage Facility

J. D. Bernardin*, S. Hopkins, W. S. Gregory, L. Parietti, D. H. Bultman, and R. A. Martin

Engineering Sciences and Applications Division - Design Engineering, Los Alamos National Laboratory, Los Alamos, NM 87545

Abstract – The Nuclear Materials Storage Facility (NMSF) at the Los Alamos National Laboratory is being renovated for long-term storage of canisters designed to hold heat-generating nuclear materials such as powders, ingots, and other components. The continual heat generation within the canisters necessitates a reliable cooling scheme of sufficient magnitude which maintains the stored material temperatures within acceptable limits. The primary goal of this study was to develop both an experimental facility and a computational fluid dynamics (CFD) model of a subsection of the NMSF which could be used to observe general performance trends of a proposed passive cooling scheme and serve as a design tool for canister holding fixtures. Comparisons of numerical temperature and velocity predictions with empirical data indicate that the CFD model provides an accurate representation of the NMSF experimental facility. Minor modifications in the model geometry and boundary conditions are needed to enhance its accuracy, however, the various fluid and thermal models correctly capture the basic physics.

---

* Author to whom all correspondence should be addressed.

NOMENCLATURE

A	area
F	forcing function
h	total heat transfer coefficient
q	heat transfer rate
T	temperature
y	dependent variable

subscripts

inf	average value within storage pipe air
new	corrected model value
old	original model value

INTRODUCTION

Background

The Nuclear Materials Storage Facility (NMSF) at the Los Alamos National Laboratory is being renovated for long-term storage of containers designed to hold heat-generating nuclear materials such as powders, ingots, and other components. In particular, the NMSF renovation involves storing nuclear materials in PF-4 stainless steel canisters (0.127 m (5.0 in.) outer diameter, 0.254 m (10 in.) length) which would in turn be stored within vertical steel tubes (0.46 m (18 in.) outer diameter, 4.27 m (14 ft) length) located underneath the working floor of the facility. Each PF-4 canister is designed to generate at most 15 W of thermal energy. The top loaded storage tubes, having a holding capacity of 14 canisters, would thus need to dissipate a total of 210 W. The entire facility will consist of an approximate 11 by 62 array of these storage tubes.

The continual heat generation within the canisters necessitates a reliable cooling scheme of sufficient magnitude which maintains the stored material temperatures within acceptable limits. Due to the high radioactivity and security issues associated with the stored materials, a fully-passive, buoyancy-driven air flow system has been analyzed and recommended for the ventilation cooling scheme [1]. The heat produced by the nuclear

materials will generate a buoyant flow which will draw cool air from inlets at one end of the storage array and exhaust the heated air out through a stack located at the opposite end.

One of the major tasks proposed in the NMSF renovation project is to design canister holding fixtures for use inside the storage pipes. These fixtures must allow for accurate insertion and removal of the canisters while at the same time, enhance the heat removal process. To aid in the fixture design process, a full-scale experimental facility, used to emulate a subsection of the NMSF, was constructed. This facility allowed general performance trends of the passive cooling scheme to be observed for a range of operating conditions. In addition, the experiment provided valuable test data for bench marking a computational fluid dynamics (CFD) model of the NMSF experimental facility. This model, developed using the software package CFX, is intended to serve as a valuable design and optimization tool for future canister fixture development. This paper summarizes both experimental and analytical results obtained in support of the NMSF canister fixture design.

Literature Review

This literature review serves as a brief introduction to computational fluid dynamics theory as well as applications to three-dimensional enclosures as they apply to the current study. While it does not serve as an in-depth review of CFD, several comprehensive references are cited.

CFD refers to simultaneous numerical solution of the continuity, momentum, and energy equations for a flow field with specified boundary conditions. Two general mathematical approaches, finite difference, and finite element have commonly been used to solve these equations [2,3]. CFX, the commercial CFD package employed in this study, uses a finite volume (finite difference) scheme based on the SIMPLEC mathematical algorithm discussed by Van Doormaal and Raithby [4]. A thorough and well written description of the predecessor to this algorithm, SIMPLE, is given by Patankar [2].

CFD methods have been used extensively and have become common-place in fluid and heat transfer problems associated with large enclosures. Some of the current

methods of research and design associated with airflow in large rooms are discussed by Nielsen [5] including the benefits and downfalls of both full and scaled experiments as well as three-dimensional CFD approaches. Aboosaidi et al. [6] employed two CFD codes, FLUENT and BINS3D, to model isothermal three-dimensional air flow patterns in aircraft cabins. Comparisons of their numerical predictions to experimental measurements consisting of smoke stream lines and hot wire anemometry velocity measurements showed promising results. While general flow field patterns were predicted quite well, velocity predictions were generally off by more than 25%. This error could have been the result of inaccuracies in geometry modeling, too coarse of a mesh, or incomplete convergence of the computer simulations. Weathers and Spitler [7] developed their own code and used it to compare CFD simulations to experimental measurements of airflow in a large room (4.6 m by 2.7 m by 2.7 m) with isothermal walls. Using different turbulence models and a defined global error parameter, they also compared trade-offs between accuracy and computational times. As with the results of Aboosaidi et al., Weathers and Spitler's code predicted general flow patterns, but its ability to predict local velocity values with a high degree of accuracy is questionable. Jacobsen and Nielsen [8] presented CFD velocity profiles for a room containing heat sources, however, lack of experimental results and a poor discussion of the numerical results severely limits the integrity of the study.

CFX, the CFD code employed in the present study, was used extensively to determine the feasibility of a passive cooling scheme for the entire NMSF [1] as well as predicting buoyant air flow patterns and temperatures in a heat-producing explosives storage chamber (12m by 3.7 m by 2.9 m) [9]. In addition, Parietti et al. [10] used CFX to model the ventilation system for the PHENIX Detector at Brookhaven National Laboratory. The solver parameters used to describe the flow field and heat transfer processes in that study were nearly identical to those in the present investigation with the exception of radiation heat transfer which was not included in the former.

In addition to serving as a basis for the NMSF canister fixture development, this study also provides valuable insight into the use of CFD models to simulate the flow and thermal fields within large enclosures. Far too often, computer simulations are accepted without substantial verification of the numerical results. Experimental measurements

required to support the computational efforts are either lacking or nonexistent, especially for relatively large scale problems. This paper reveals the accuracy, usefulness, and limitations of a CFD model by providing extensive comparisons between numerical and experimental velocity and temperature data.

EXPERIMENTAL METHODS

The NMSF Experimental Facility shown in Fig. 1 was constructed to investigate the proposed passive cooling scheme and provide experimental data to support numerical modeling efforts. The experimental configuration was designed to simulate the performance of a single storage pipe rather than the entire NMSF. As such, the experimental facility consisted of in part, a single full scale steel storage tube containing a string of 14 Plutonium Facility (PF-4) stainless steel canisters. Each canister contained an electrical resistance flexible silicon mat heater to provide 15 W (±10%) of thermal energy which simulated the heat generation of the nuclear materials. Each can was individually wired to a separate power supply for accurate control of the power input. For the preliminary tests, the canisters were strung together with a steel braided cable and centered along the axis of the steel storage pipe. Access to the pipe for placement of the canisters and instrumentation was provided through the top, while the bottom of the pipe was welded to a large steel floor plate. Type T thermocouples (calibrated to ±0.5 °C) were positioned at various locations as noted in Fig. 2 to monitor temperatures of the can surfaces, internal pipe air, pipe wall and external pipe air. A Gateway 2000 computer and a Hewlett Packard data acquisition system operating with Labview software were used to read and store the temperature data.

Located to the front and back of the instrumented pipe with respect to the horizontal airflow direction, were two dummy cardboard pipes. These dummy pipes were installed as a means of partially developing the air flow induced on the system. Two insulated vertical walls on either side of the three pipes as well as an insulated ceiling plate formed the outer boundaries of the air flow passage. The steel base plate was also insulated and contained a 115 W electrical resistance guard heater to minimize heat conduction losses from the storage pipe. To simulate the larger facility as closely as

feasible, the surrounding walls were positioned at symmetric boundaries corresponding to those which would exist if an entire array of tubes were present. In addition, all surrounding walls and dummy tubes were insulated and covered with a highly reflective foil to further simulate the radiation imposed on a single storage tube from its surrounding neighbors. Eight Dayton axial blowers (Model 4C447, 110V, free air 265 CFM) were evenly positioned at the inlet side of the facility. Immediately downstream of the blowers were a series of flow straighteners consisting of arrays of horizontal cardboard tubes (5.08 cm (2 in.) diameter , 45.72 cm (18 in.) length) in series with a layer of 1.27 cm (0.5 in.) thick open cell foam sheet and 2 sets of wire screen mesh (18 by 15 wires/in^2). A hot wire anemometer was employed to insure that deviations in the outlet velocities across the exit cross-section of the flow straighteners were within 10% of the mean velocity. This anemometer was also used to measure air velocities at the most-downstream dummy tube during operation (±10%). Access and equipment limitations prevented a complete set of velocity measurements throughout the facility.

Testing commenced with turning on the canister and base plate heating elements and monitoring the can temperatures. For flow tests, the blowers were turned on when can temperatures approached anticipated steady-state values. The entire system required at least 24 hours to reach thermal equilibrium, after which the steady-state temperature data was taken. For each set of operating conditions, the experiment was repeated at least once to insure reproducibility.

NUMERICAL METHODS

The numerical analysis of the operating performance of the NMSF (experimental facility) involved simultaneously solving the continuity, Navier-Stokes (momentum), and energy equations. The three dimensional modeling conditions included steady-state buoyant and turbulent flow, as well as conduction, convection, and radiation heat transfer. In addition, since the temperature and density variations were relatively small, the Boussinesq approximation could be made thus allowing the air to be modeled as incompressible. The ability of the commercial CFD program CFX to solve this coupled and large scale problem made it ideal for the present study. In addition, CFX is an

industry-driven code that has been developed under ISO 9001 requirements and has been validated with numerous test problems.

CFX is a finite volume, implicit Navier-Stokes solver that uses a revised version of the mathematical algorithm Semi-Implicit Method for Pressure-Linked Equations (SIMPLE) [2] termed SIMPLEC [4]. In addition, the code uses several well-developed differencing schemes to discretize the derivatives in the governing differential equations [11]. A discrete Shah radiation model [12] with single radiation zones formed from approximately 62 elements was employed to solve for the radiation heat transfer contribution. Turbulence created by the buoyant flow was predicted with a two-equation K-ε model. CFX default values for K and ε. were used and sensitivity studies on the values of the turbulence parameters were left as future work. All numerical simulations were run on an SGI Indigo workstation with a 256 Mb RAM, 250 MHz IP22 processor, MIPS R4010 Rev 0 floating point chip, and a MIPS R4400 Rev 6.0 processor chip.

Model Geometry, Grid, and Boundary Conditions

The geometrical model for the numerical simulations is shown in Fig. 3. For the most part, the geometrical model closely emulates the experimental facility. However, to limit the model's mesh size and computational time and yet still provid a meaningful representation of the experimental facility, the series of canisters was modeled as a continuous cylinder with a uniform heat flux. This is a fairly good assumption considering the distribution of the heat flux provided by the flexible heaters in the experimental facility. A more detailed model which accounts for the air gap between cans has been deferred to a later modeling effort which will focus on canister fixture designs.

The grid generator for CFX uses a multi-block scheme with a body-fitted grid structure. The grid used for the geometrical model is shown in Fig. 4. A total number of 474,000 elements were generated, with 100 cells in the vertical direction, and a varying distribution in the horizontal plane depending on the accuracy required in a given region. For example, boundary layer thickness calculations for the can surfaces were performed

to insure that several cells encompassed this high temperature and velocity gradient region.

Air at atmospheric pressure and 22 °C was used as the cooling medium. Experimental measurements showed the inlet velocities from the blowers deviated less than 10% from the mean value, thus justifying using a uniform inlet velocity in the numerical model for the low-flow case. For the non forced flow case, with no air delivered from the blowers, atmospheric pressure boundaries were defined at the inlet and outlet. The structure of the geometry and boundary conditions allowed simplification of the numerical model by placing a line of symmetry down the center of the model from the inlet to the outlet. The symmetry modeling scheme prevents capturing unsteady vortices, however, the low magnitude of the external air velocities and close packing arrangement of the storage tubes was believed to prevent the formation of such phenomena. Next, perfect insulation was assumed on all walls surrounding the storage pipe, including the dummy tubes. This is very reasonable since the actual surfaces were insulated with a 1.27 cm (0.5 in.) thick foam insulation. Finally, total, hemispherical emissivity [13] and surface roughness values were applied to the boundaries of the geometrical model. The specific values of these parameters are given in Fig. 3.

RESULTS

To determine the accuracy and credibility of the force and non-forced air flow CFX models, a four-step validation procedure of the numerical solution was employed. First and foremost, the convergence of a particular model onto a solution was determined with *residuals*. In the solution algorithm of CFX, each dependent variable, y, (i.e. temperature) is solved for in algebraic equations of the form

$$f(y) = F \tag{1}$$

where F is a forcing function.

The residual for the dependent variable y, is the error or difference between the left and right hand sides of equation (1). The residuals for each dependent variable were

determined at each cell and summed over all cells for a single iteration. A converged solution was obtained when the sum of the residuals for each dependent variable ceased to vary between consecutive iterations.

The next two tests of convergence were mass and energy balances of the system. For the steady-state problems considered in this study, convergence was assumed when there was less than a 5% difference in the inlet and outlet flows of mass and energy.

The final verification of the numerical models was achieved with experimental validation, in which empirical velocity and temperature data were compared with numerical predictions.

Non Forced Air Flow

Figure 5 displays the temperature contours of the canisters, inner storage pipe air, and external air flow passage outermost surfaces within the NMSF model for the non forced air flow test case. The canister surfaces represent the hottest locations in the system with temperatures ranging roughly between 40 and 58 °C while inner pipe air temperatures are roughly 28 °C at the bottom of the facility and nearly 45 °C near the top. Due to the extensive cooling air volume and relatively low pipe wall temperatures (approximately 30 °C), the external air temperatures remain below 28 °C (ambient temperature is 22 °C). Further details of the temperature distributions can be inferred from Figures 6 and 7 which display, respectively, the temperature contours on the storage pipe's inner surface and the buoyant thermal plumes developed outside the storage pipe. From these temperature contour plots, several general observations concerning the fundamental operation principles of the passive cooling system can be made. First, a buoyancy driven flow within the storage pipe supplemented with radiation, removes heat from the canister surfaces and delivers it to the pipe wall. The pipe wall in turn develops a vertical buoyant flow in the external air chamber and also radiates heat to the surrounding walls. In both cases, the air is continuously heated as it rises to the top of the facility resulting in increasing canister surface temperatures with elevation. The buoyant air flow patterns established in and outside the storage pipe are further described by velocity vector plots in Fig. 8. The external air flow is seen in Fig. 8a to originate from

the heated pipe wall and then exit out the top sections of the left and right side openings of the facility. Not displayed in the figure are inlet flows established at the lower portions of the left and right side openings which feed the buoyant plume around the central storage pipe. Fig. 8b shows the recirculating flow within the storage pipe. The hot air at the canister surface flows vertically to the top of the facility, where it is directed outward and then down along the pipe wall where it is continuously cooled. Also shown in Fig. 8b is the vertical air flow established on the outside of the storage pipe and discussed previously.

Forced Air Flow

Figure 9 displays the temperature contours of the canisters, inner storage pipe air, and external air flow passage outermost surfaces within the NMSF model for the forced air flow test case. The temperature magnitudes and distribution are quite similar to the non forced flow results of Fig. 6, thus indicating that heat transfer is primarily driven by free rather than forced convection for the conditions studied. The flow patterns around the canisters and storage pipe are shown in Fig. 10a for a vertical plane near the center line of symmetry. The symmetrical air flow pattern inside the storate tube is nearly identical to that described in Fig. 8b for the non forced air flow case. The buoyant flow on the outside of the storage pipe, however, is unsymmetrical, unlike the pattern developed in the non forced flow case. This flow pattern is the result of the horizontally forced air flow which causes recirculation on the downstream sides of the dummy and storage pipes as shown in the velocity vector plot of Fig. 10b.

The air flow and associated temperature patterns predicted with the NMSF model are consistent with intuition for both flow test cases and, as will be seen in a later section, agree quite well with experimental measurements.

Model Validation

Figure 11 compares the numerical model temperature predictions with the experimentally measured values for the non forced air flow test case. The pipe wall and both internal and external air temperature predictions agree quite well with empirical values with an accuracy of better than 10% for the most part. It is speculated that heat

losses in the experimental facility caused the experimental temperatures to be slightly lower than the predicted values. The canister temperature predictions exhibit the same elevation dependency as the experimental values but possess errors in the range of 15 to 20%. Figure 12 displays the same type of information but for the forced flow condition. Again, the pipe wall and air temperature predictions show excellent agreement with empirical values, while the canister temperature predictions exhibit errors with the same magnitude range as in Fig. 11. Table 1 presents a comparison between numerical and experimental air velocities for the forced flow test case at various elevations in the external air flow passage between the downstream dummy tube and outer wall. Excellent agreement was obtained for all locations except for the measurement closest to the floor. It is believed that the storage pipe mounting gussets in the experimental facility greatly restricted the flow, consequently providing a significantly lower air velocity than predicted.

The differences in the numerical and experimental canister surface temperatures were discovered to lie in the method used to model the canister geometry. In the numerical model, the series of canisters was modeled as a continuous pipe with a uniform heat flux provided by 210 W of input energy. While this same 210 W was supplied to the canisters in the experiment, the surface area over which the heat was dissipated was different than that used in the model since the canisters were separated by a 5.08 cm (2.0 in) gap. Assuming that the heat was dissipated solely by the outer side surface of the canisters in the experiment, then 20% less surface area would be available to dissipate the 210 W of thermal energy in the experiment compared to the model. This indicates then that a 80% lower heat flux exists in the numerical model, and hence predicted canister surface temperatures would be significantly less than experimental values. To determine the magnitude of the canister temperature discrepancy produced by differences in heat transfer area in the model and experiment, a corrective scheme which accounted for the area difference was adapted. Assuming that the total heat transfer rate for the old or original model, q_{old}, was equal to that of the new or corrected model, q_{new}, but the area over which this heat transfer occurred was different,

$$q_{new} = q_{old} \tag{2}$$

or

$$h\,A_{new}\,(T_{new} - T_{inf}) = h\,A_{old}\,(T_{old} - T_{inf}), \tag{3}$$

then the corrected model canister temperatures are given by

$$T_{new} = A_{old}/A_{new}(T_{old} - T_{inf}) + T_{inf}. \tag{4}$$

Figure 13 displays the corrected model canister temperatures for the non forced air flow case as determined with equation (4) using an average internal air temperature of 35 °C for T_{inf}, the originally predicted canister temperatures, T_{old}, of Fig. 11, and the corrected heat transfer area equal to the outer canister surface area found in the experiment. The error in the model predictions is seen to be reduced by approximately 50%. The remaining discrepancies are most likely due to differences in radiation properties of the model and experiment, as well as non uniformities in the experimental heat fluxes caused by uneven surface coverage of the canister resistance heaters. To alleviate the temperature discrepancies and hence provide increased accuracy in the design of the canister holding fixtures, several modifications to the numerical model are currently being implemented.

CONCLUSIONS

The primary goal of this study was to develop both an experimental facility and a CFD model of a subsection of the NMSF. The experiment allowed general performance trends of a proposed passive cooling system to be observed while also supplying vital empirical data needed to benchmark the CFD model. Comparisons of numerical predictions with empirical data indicate that the CFD model provides an accurate representation of the NMSF experimental facility. Minor modifications in the model geometry and boundary conditions are needed to enhance its accuracy, however, the various fluid and thermal models correctly capture the basic physics. This modified numerical model will be employed in the future design and optimization of canister

holding fixtures for the storage pipes of the NMSF. In addition, the successful modeling accomplishments of the single storage pipe presented in this study, support the development of a more complex model of the actual NMSF which includes a complete array of storage tubes. Such a model will permit investigation of the critical influence of neighboring tubes on the air flow and temperature patterns around a storage tube.

Acknowledgments

The authors greatly acknowledge the support and consulting work of the technical support staff at AEA Technology in regards to CFX modeling. This work was supported by the U.S. Department of Energy.

REFERENCES

[1] Gregory, W. S., 1995, "NMSF Heat Removal Analysis," Technical Report, Los Alamos National Laboratory, TSA8-LA-20.

[2] Patankar, S. V., 1980, Numerical Heat Transfer and Fluid Flow, McGraw-Hill, NY.

[3] Anderson, D. A., Tannehil, J. C., and Pletcher, R. H., 1984, Computational Fluid Mechanics and Heat Transfer, McGraw-Hill, NY.

[4] Van Doormaal, J. P. and Raithby, G. D., 1984, "Enhancements of the SIMPLE Method for Predicting Incompressible Fluid Flows," *Num. Heat Trans.*, Vol. 7, pp. 147-163.

[5] Nielson, P. V., 1994, "Air Distribution in Rooms - Research and Design Methods," Proceedings of the 4th International Conference on Air Distribution in Rooms, Cracow, Poland.

[6] Aboosaidi, F., Warfield, M. J., and Choudhury, D., 1991, "Computational Fluid Dynamics Applications in Airplane Cabin Ventilation System Design," Proceedings of the International Pacific Air and Space Technology Conference and 29th Aircraft Symposium, SAE, Warrendale, PA, pp. 249-258.

[7] Weathers, J. W. and Spitler, J. D., 1993, "A Comparitive Study of Room Airflow: Numerical Prediction using Computational Fluid Dynamics and Full-Scale Experimental Measurements," Proceedings of the 1993 Annual Meeting of the

American Society of Heating, Refrigerating, and Air-Conditioning Engineers, ASHRAE Transactions, Atlanta, GA, Vol. 99, Part 2, pp. 144-157.

[8] Jacobsen, T. V. and Nielsen, 1994, "Investigation of Airflow in a Room with Displacement Ventilation by Means of a CFD-Model," Department of Building Technology and Structural Engineering, Aalborg University, Aalborg, Denmark.

[9] Gregory, W. S., 1995, "Thermal and Airflow Analysis of Pantex 21A Stage Right Configured Modified Richmond Magazine," Technical Report, Los Alamos National Laboratory, TSA8-LA-19.

[10] Parietti, L., Martin, R. A., and Gregory, W. S., 1996 "CFD-Based Design of the Ventilation System for the PHENIX Detector," Technical Report, Los Alamos National Laboratory, LA-UR-96-2322.

[11] CFX 4.1 Flow Solver User Guide, 1995, Computational Fluid Dynamics Services, Harwell Laboratory, Oxfordshire OX11 0RA, United Kingdom.

[12] Shah N.G., 1979, "New Method of Computation of Radiation Heat Transfer in Combustion Chambers," Ph.D. thesis, Imperial College of Science and Technology, London England.

[13] Incropera, F. P. and DeWitt, D. P., 1985, Fundamentals of Heat and Mass Transfer, 2nd ed., John Wiley & Sons, NY.

Table 1. Comparison of the numerical model velocity predictions with experimentally measured values for the forced air flow test case in the center of the external air flow passage alongside the second dummy tube.

Elevation (cm)	Numerical Model Velocity (m/s)	Experimentally Measured Velocity (m/s)	Percent Error (%)
11.4	0.35	0.20	75.0
115.6	0.36	0.37	2.7
227.3	0.40	0.42	5.0
336.6	0.46	0.49	6.1
440.7	0.45	0.46	2.2

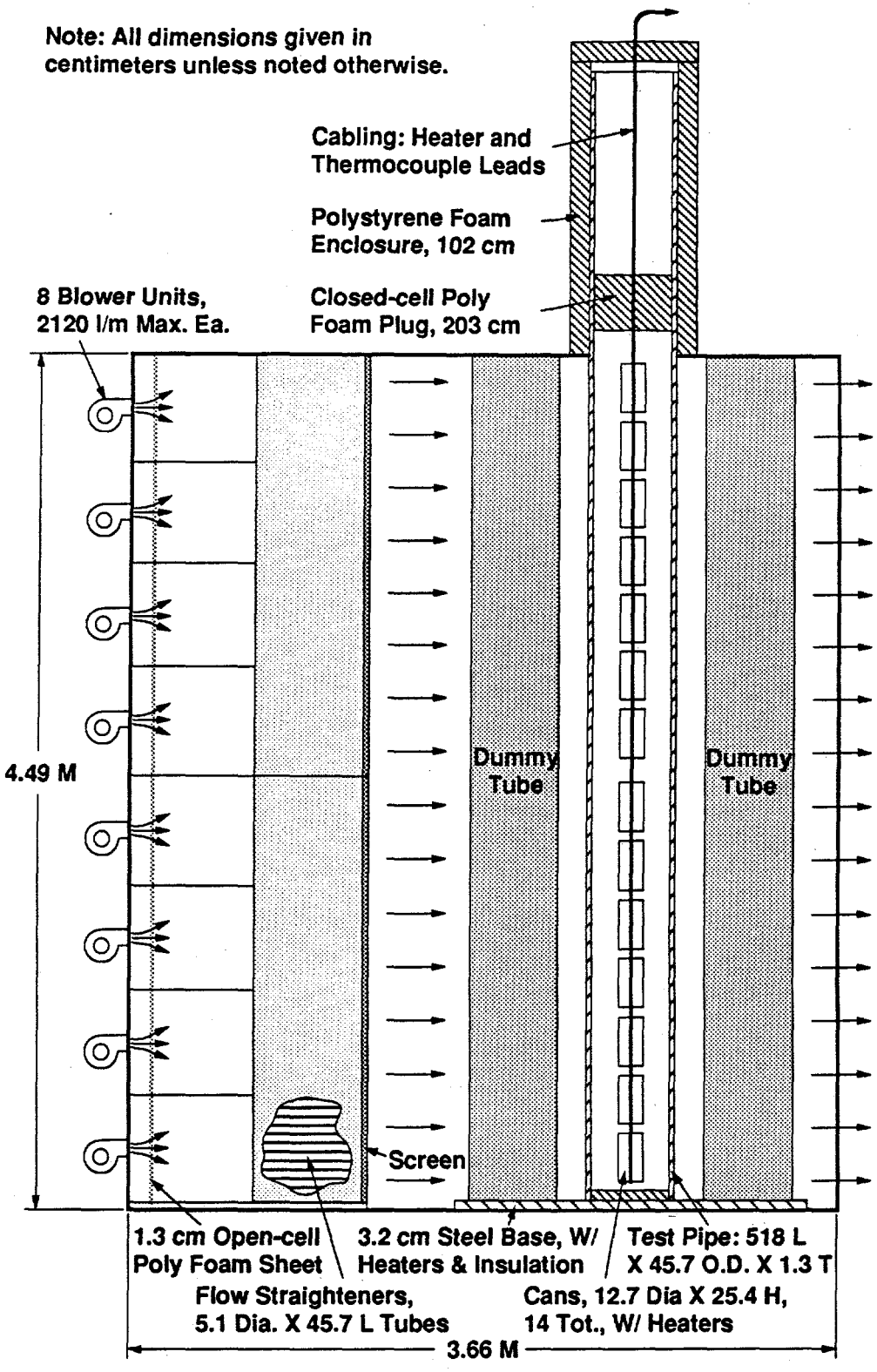

Figure 1. Schematic diagram of the NMSF experimental facility.

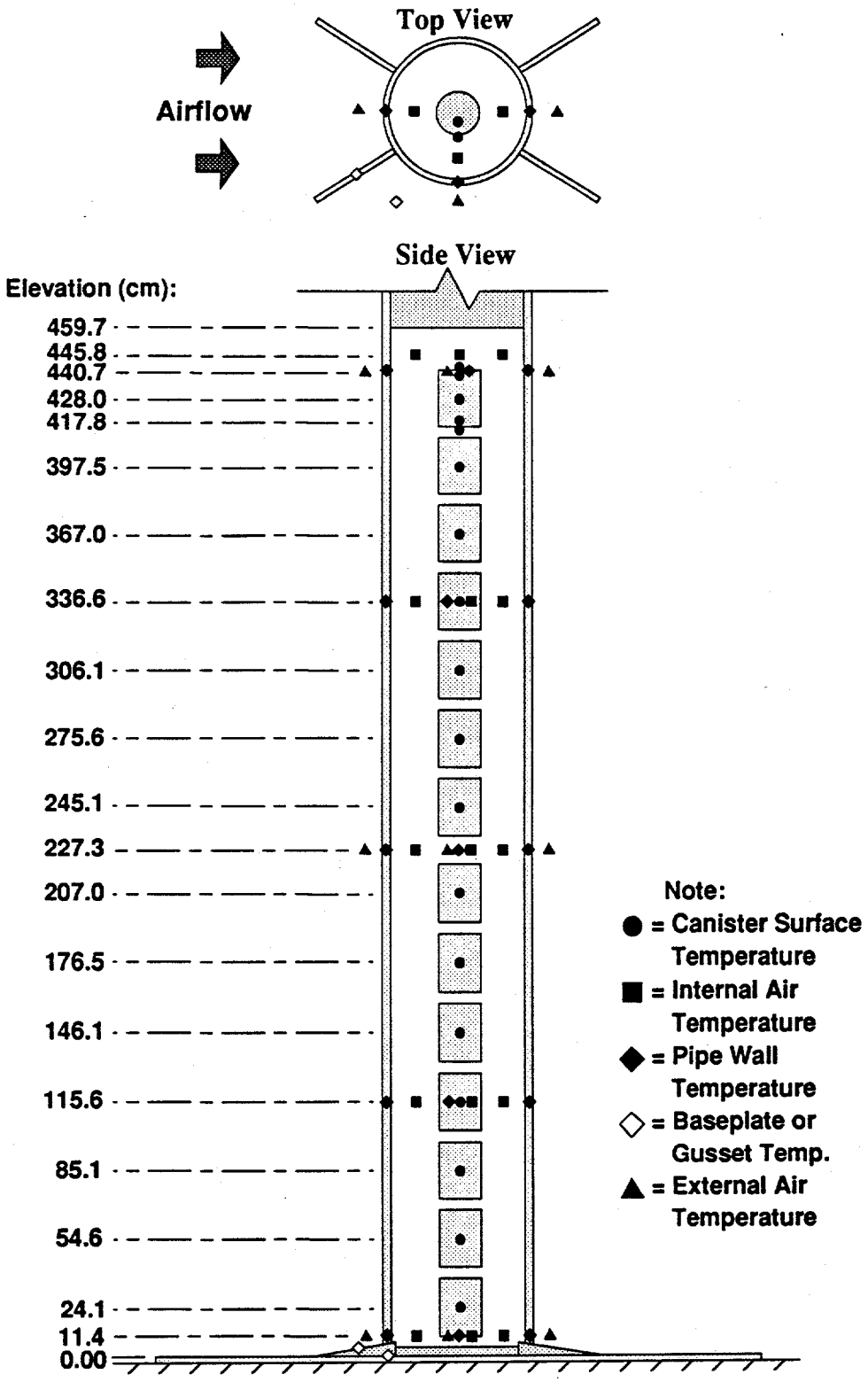

Figure 2. Schematic diagram of the instrumented canisters and thermocouple locations.

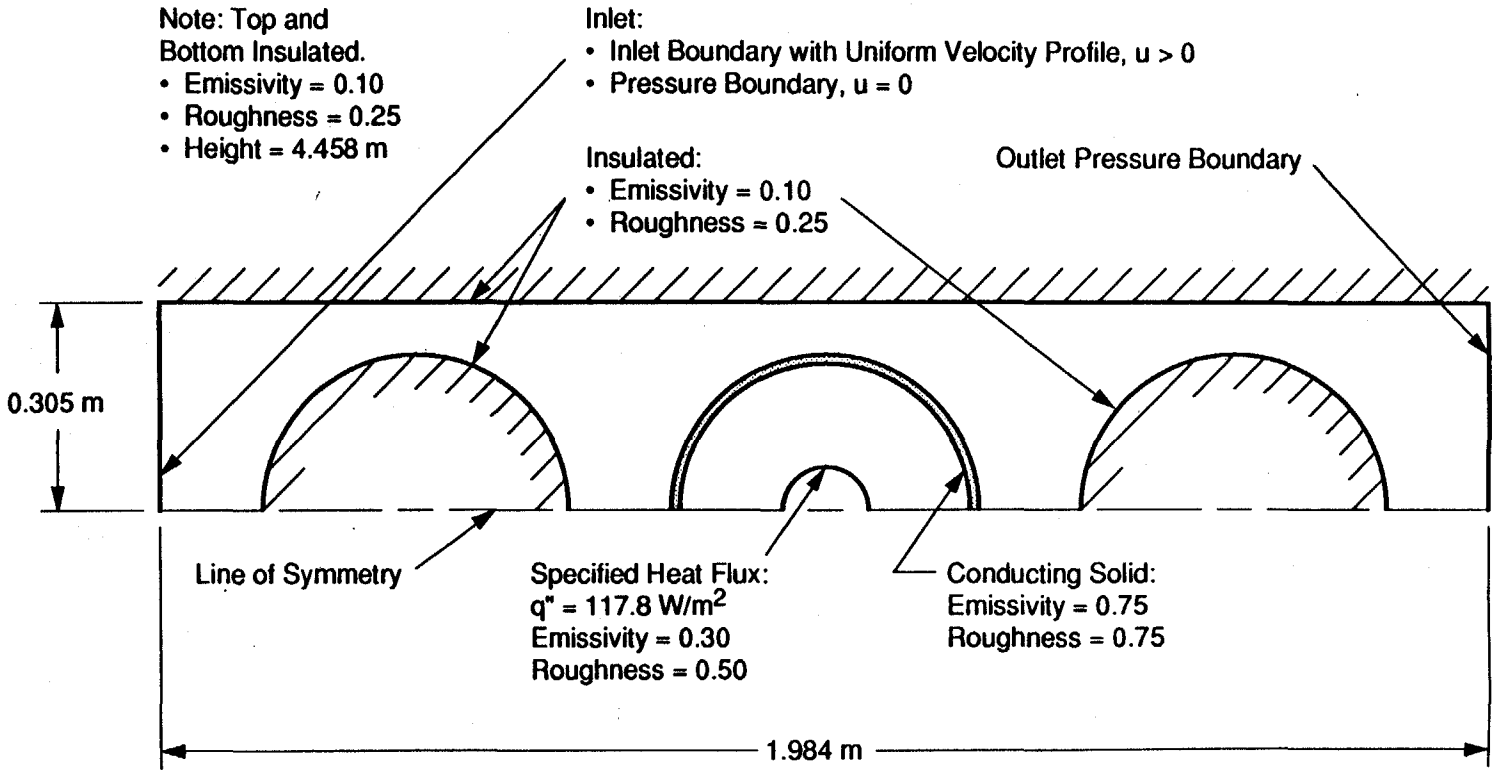

Figure 3. NMSF numerical model geometry and boundary conditions.

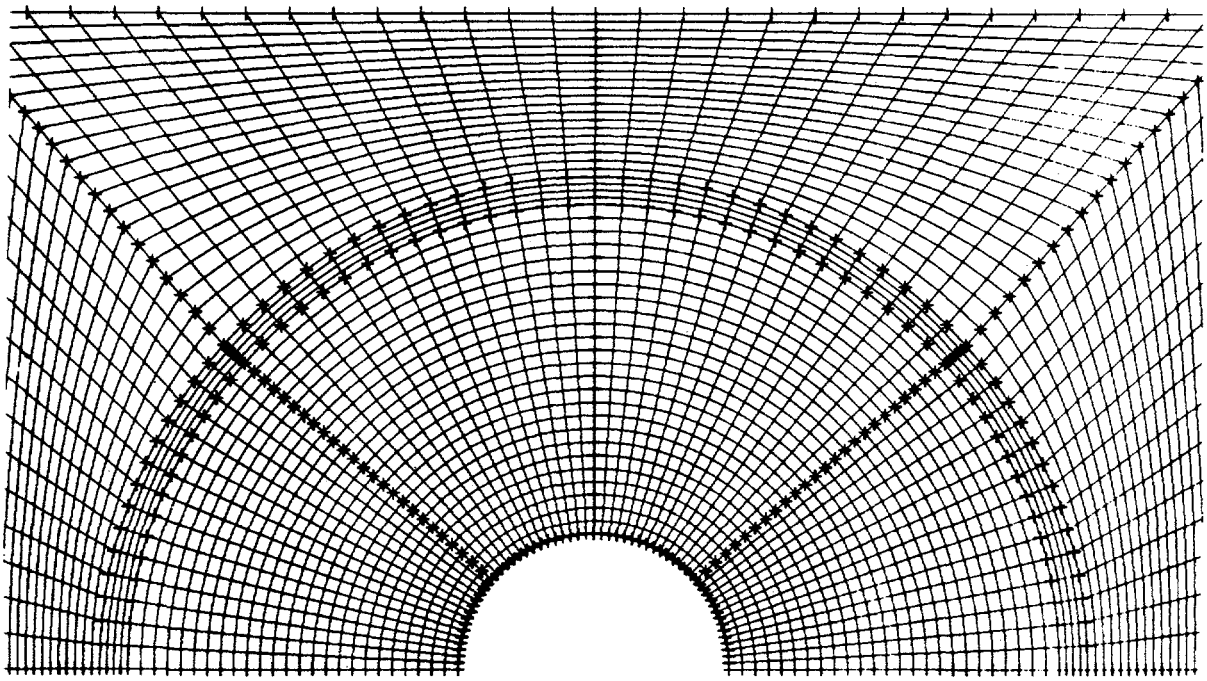

Figure 4. NMSF numerical grid mesh around the canisters and storage pipe.

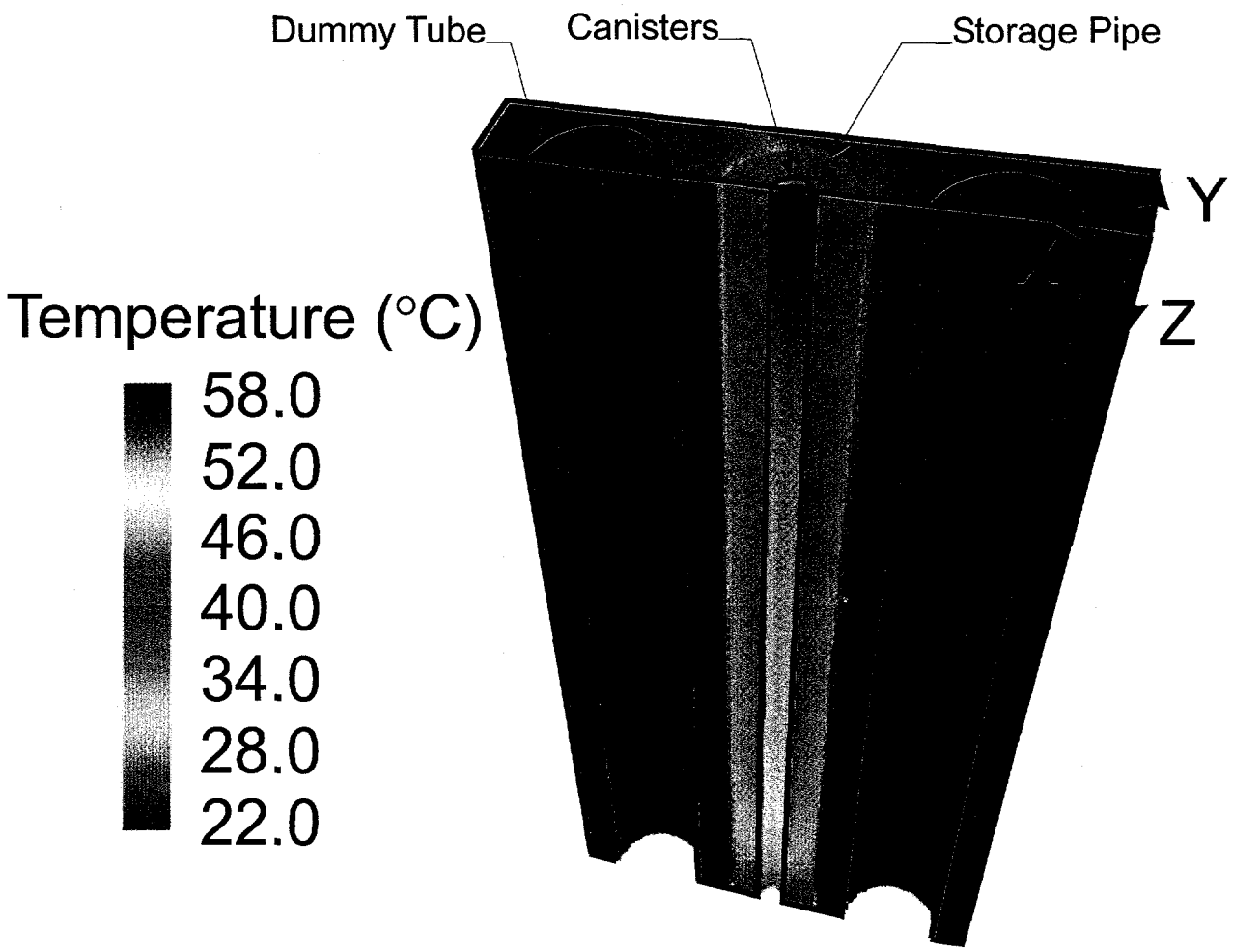

Figure 5. Numerical model temperature contours on the outermost surfaces corresponding to the non forced air flow test case.

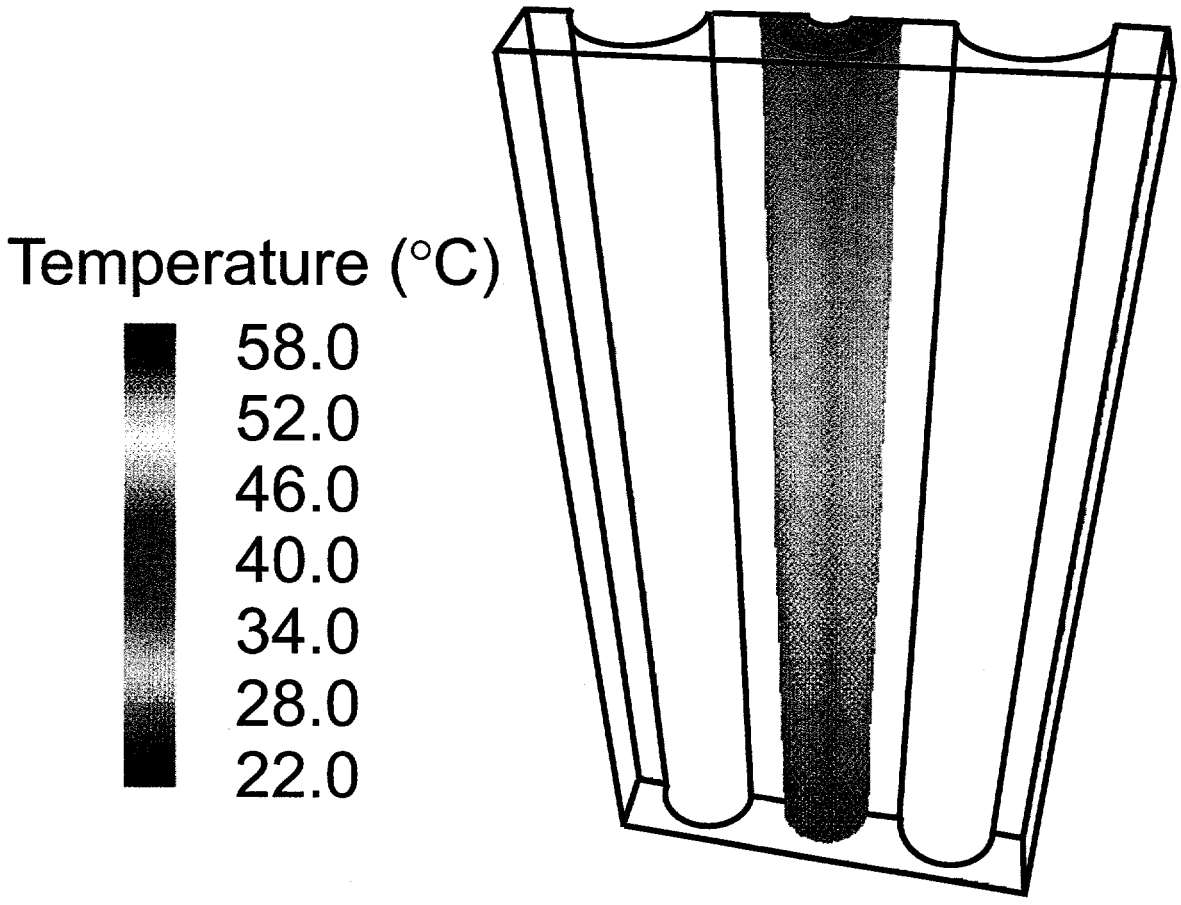

Figure 6. Numerical model temperature contours on the storage pipe's inner surface corresponding to the non forced air flow test case.

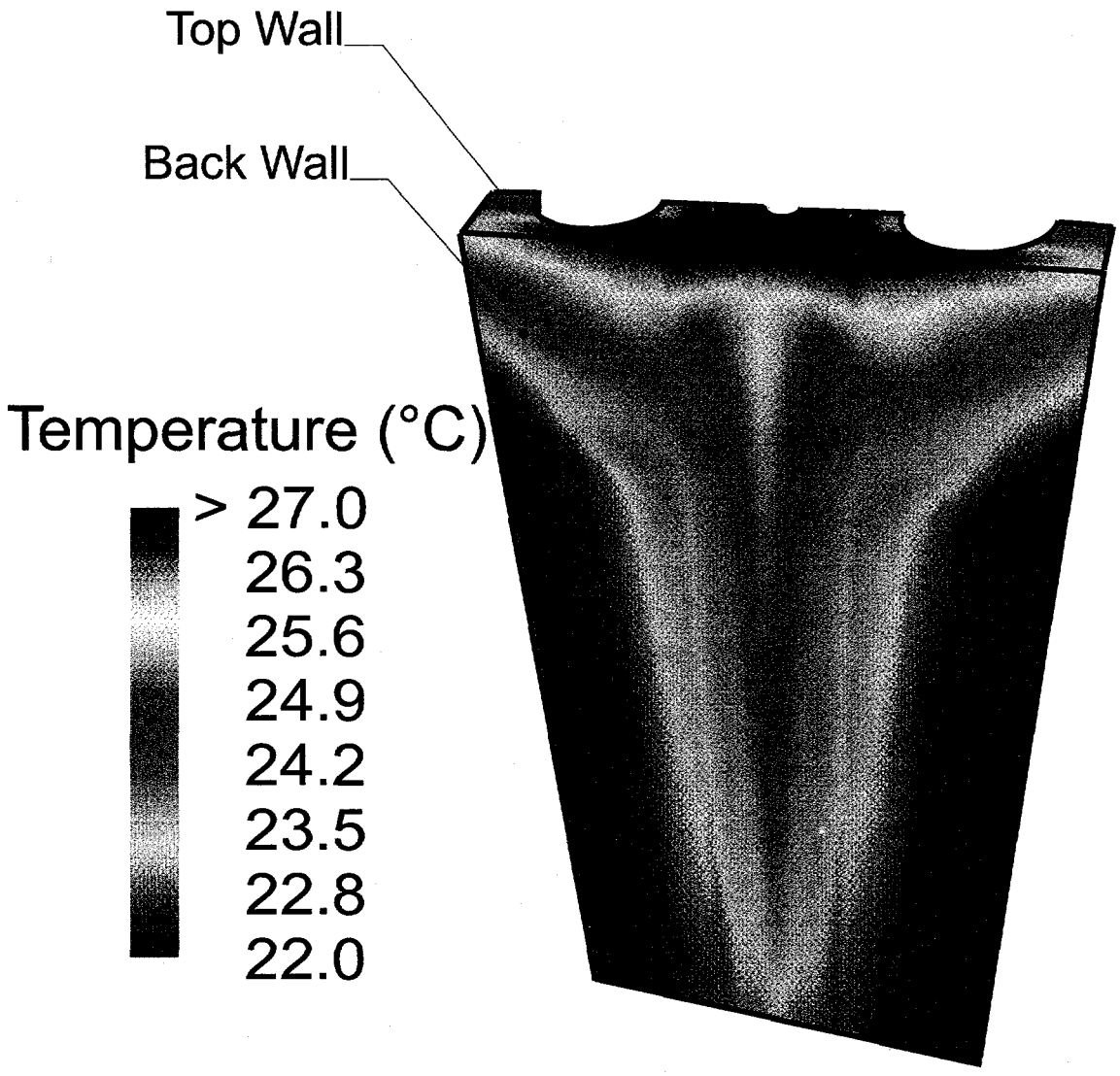

Figure 7. Numerical model temperature contours of the back and top wall surfaces corresponding to the non forced air flow test case.

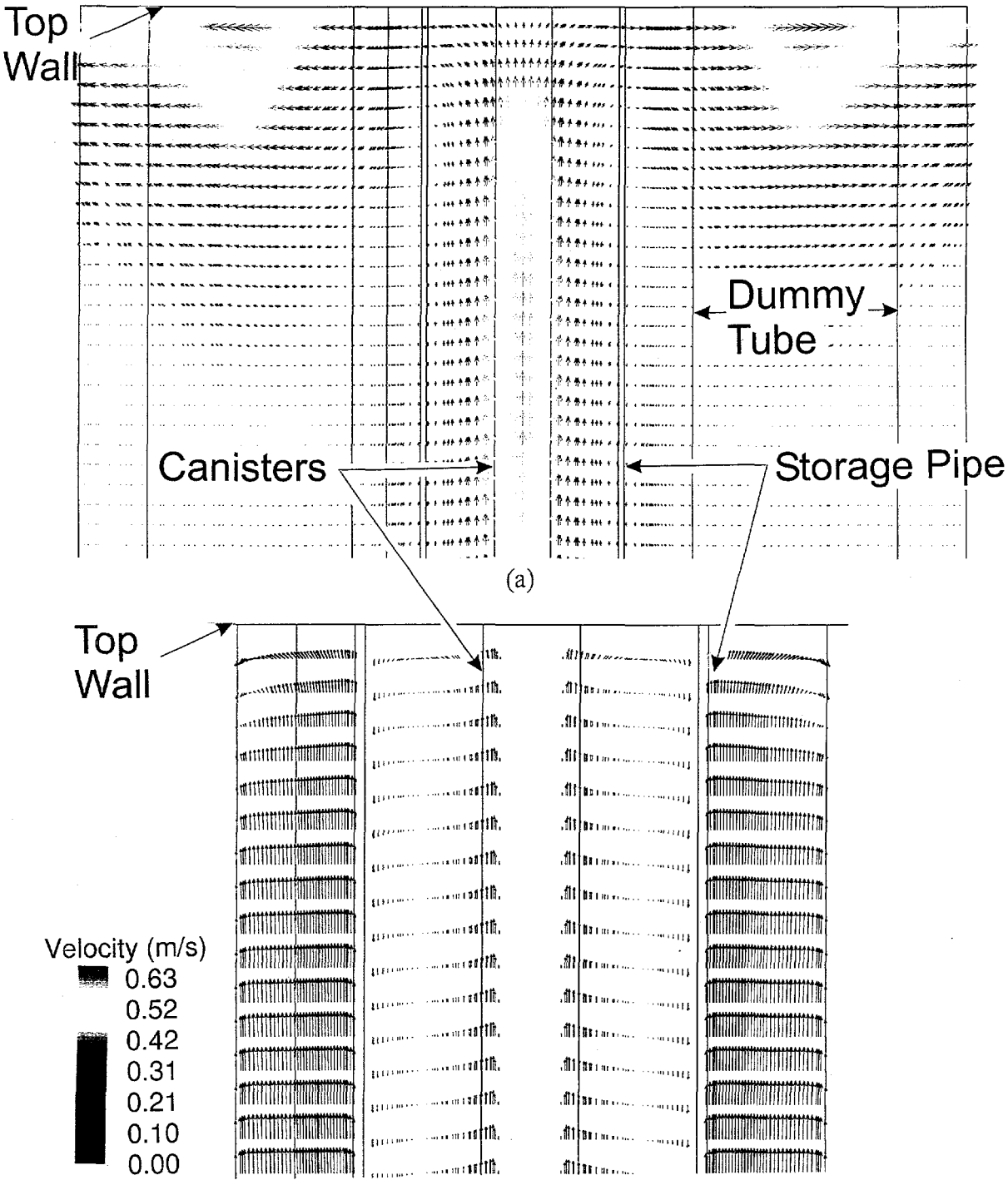

Figure 8. Numerical model velocity vector plot corresponding to the non forced air flow test case for (a) a vertical plane near the center of the external air flow passage (Y = 0.267 m) and (b) a vertical plane near the center symmetry line (Y = 0.050 m).

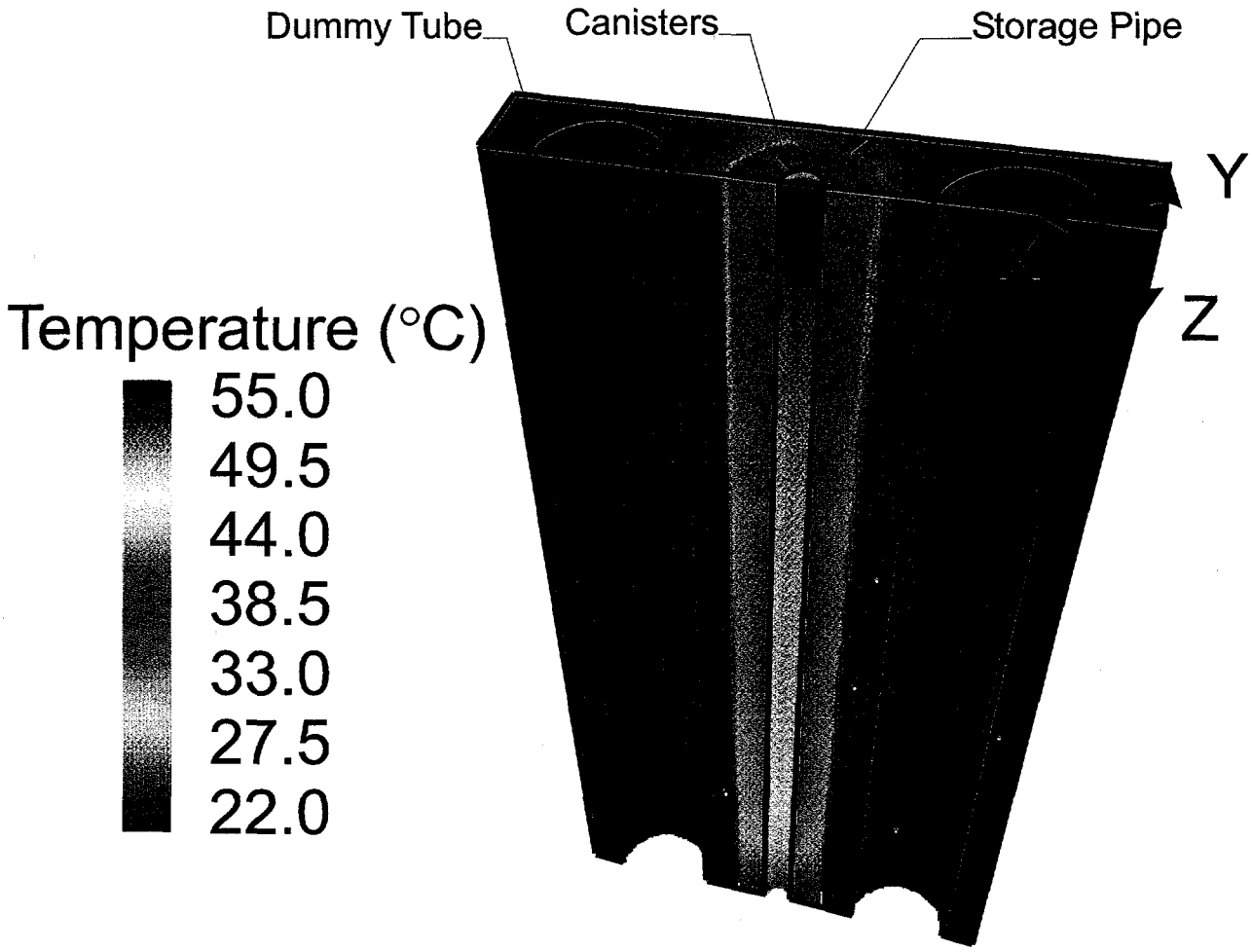

Figure 9. Numerical model temperature contours on the outermost surfaces corresponding to the forced air flow test case.

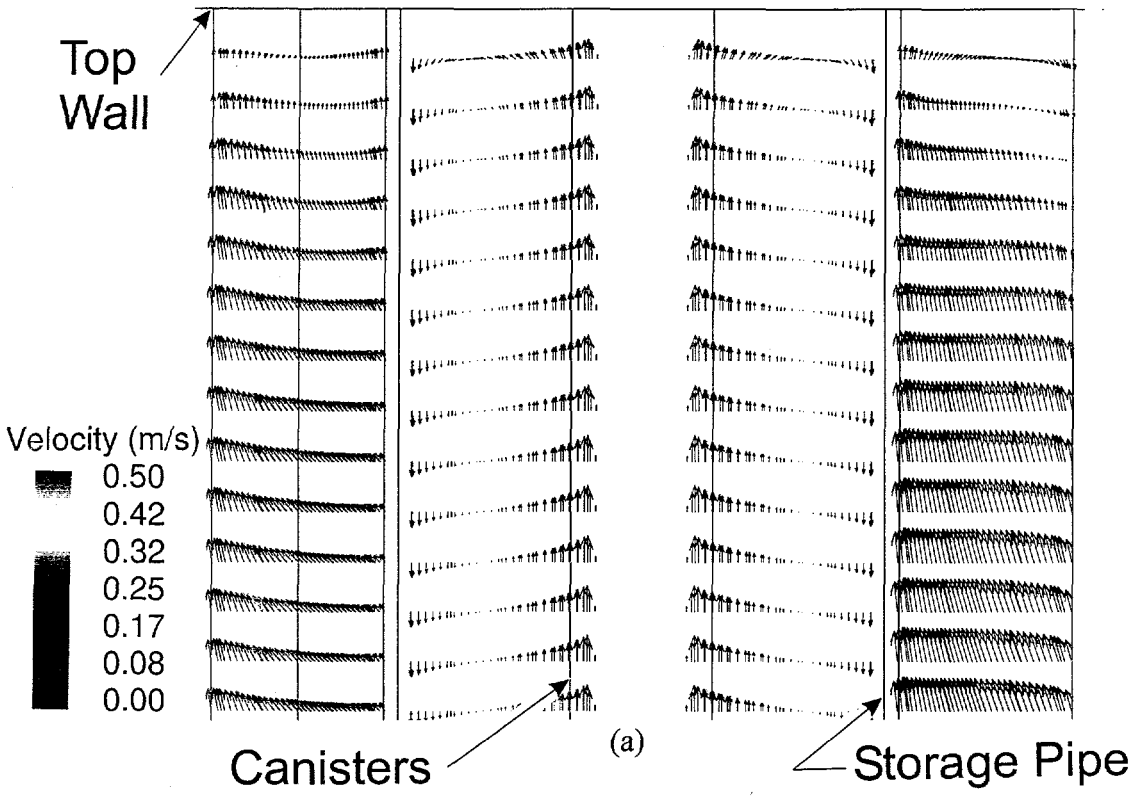

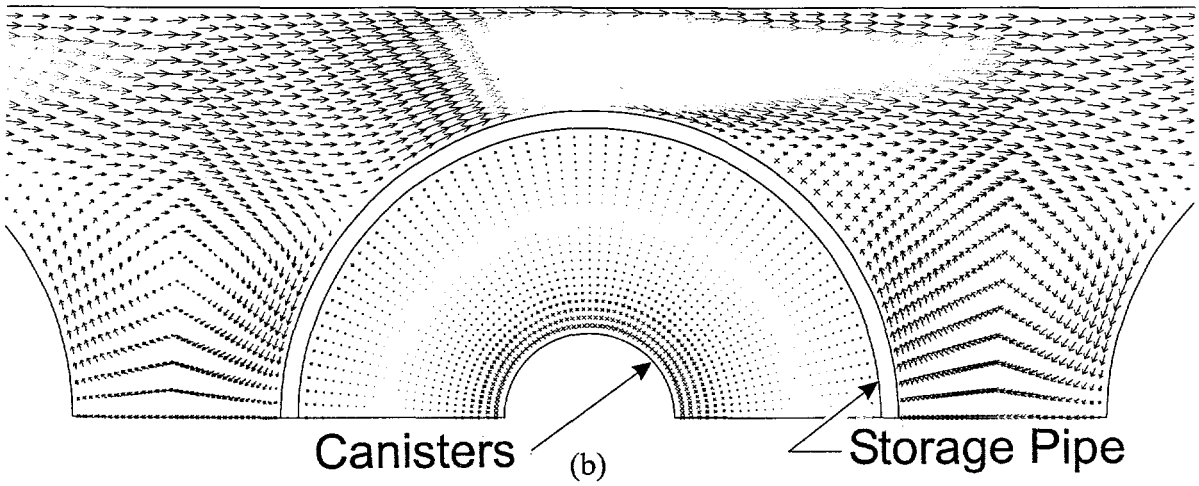

Figure 10. Numerical model velocity vector plot corresponding to the forced air flow test case for (a) a vertical plane near the center symmetry line around the storage pipe (Y = 0.050 m) and (b) a horizontal plane at the middle of the facility (Z = 2.229 m).

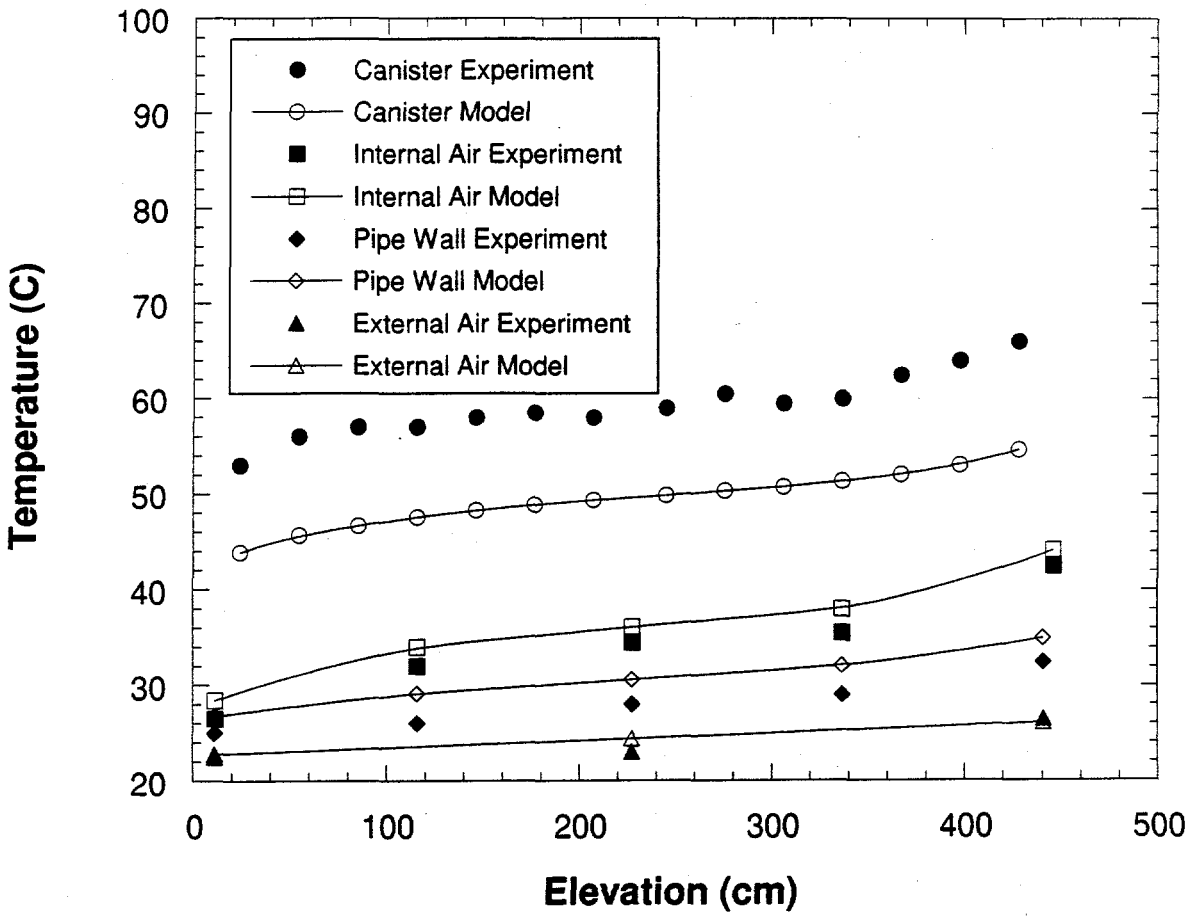

Figure 11. Comparison of the numerical model temperature predictions with experimentally measured values for the non forced air flow test case.

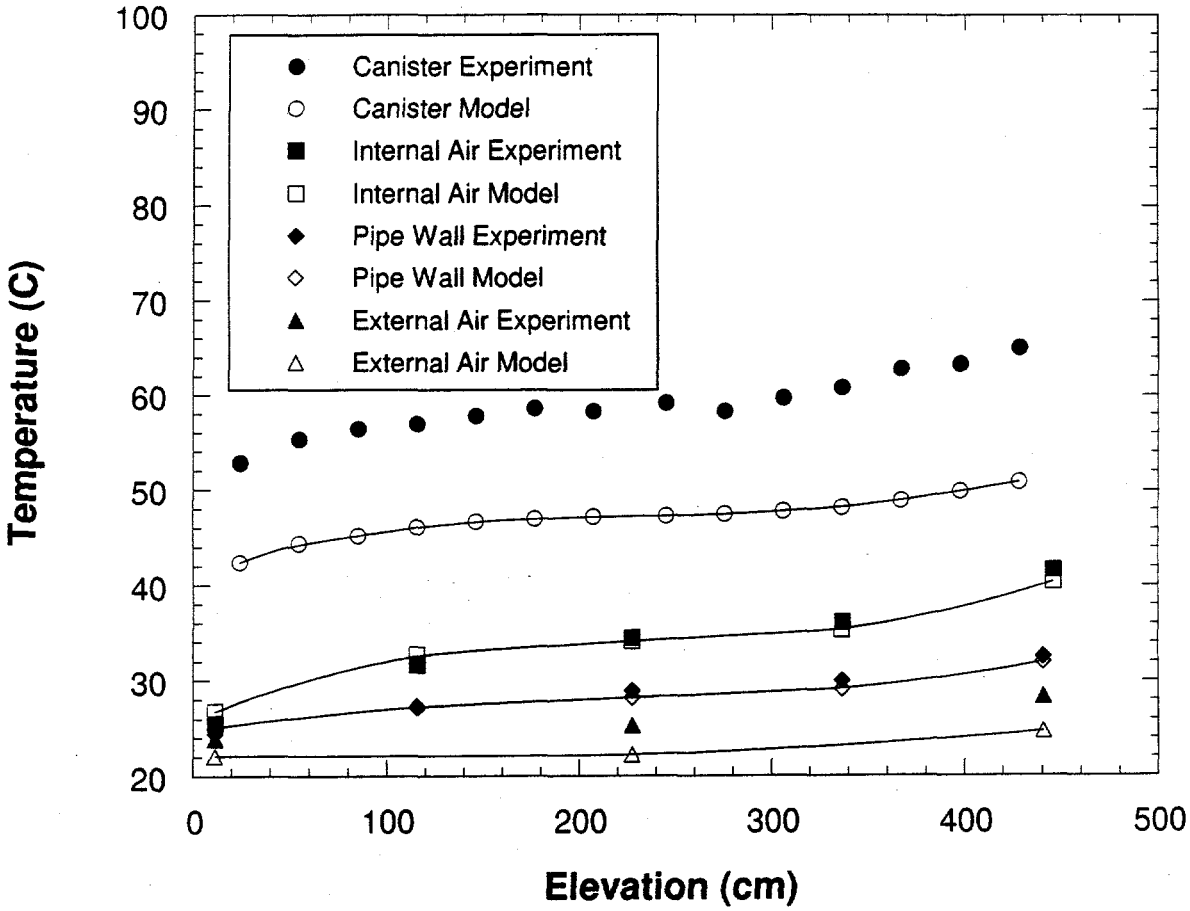

Figure 12. Comparison of the numerical model temperature predictions with experimentally measured values for the forced air flow test case.

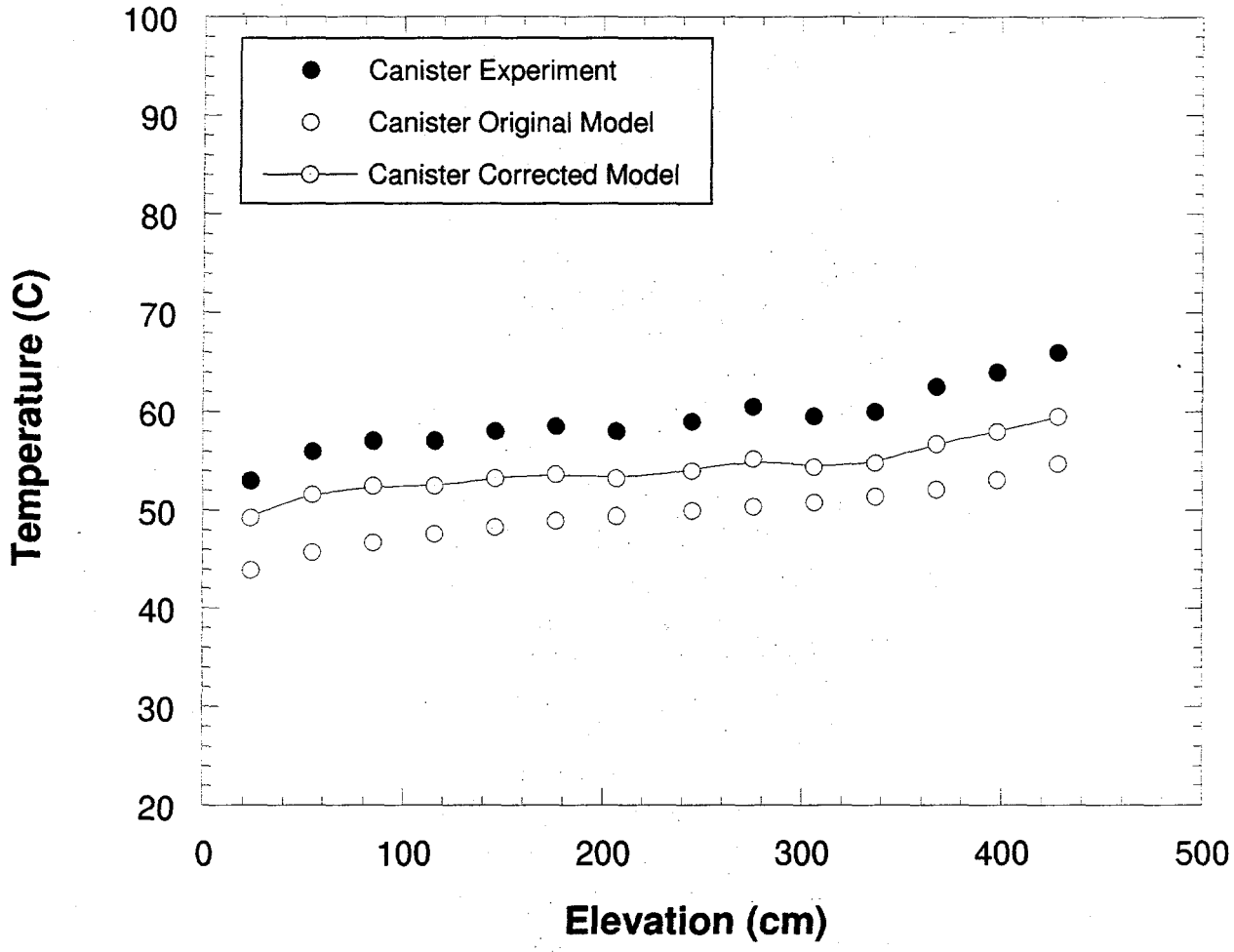

Figure 13. Comparison of the corrected numerical model canister temperature predictions with experimentally measured values for the non forced air flow test case.